Structural relaxation in silicate glasses and melts: High-temperature Raman spectroscopy

Wim J. Malfait and Werner E. Halter
Institute for Isotope Geochemistry and Mineral Resources, ETH Zurich, 8092 Zurich, Switzerland
(Received 8 June 2007; revised manuscript received 20 August 2007; published 3 January 2008)

By combining both isothermal and rate heating experiments, structural relaxation times were determined in the glass transition range with *in situ*, high-temperature Raman spectroscopy. The obtained relaxation times agree well with the shear relaxation times obtained from viscosity data. Thus, the time scale for viscous flow is the same as the time scale of the rearrangement of the silicate network structure toward chemical equilibrium. This demonstrates that Si—O bond breaking is the primary control on silicate melt viscosity.

DOI: 10.1103/PhysRevB.77.014201 PACS number(s): 64.70.P−, 61.43.Fs, 66.20.−d, 78.30.−j

I. INTRODUCTION

Thanks to several decades of intense study, a comprehensive picture of the kinetic aspects of the glass transition and structural relaxation has emerged.[1–3] For silicate melts, relaxation times around the glass transition obtained from calorimetric and volumetric measurements have been shown to be identical.[4] In addition, these relaxation times are the same as the shear relaxation times obtained from viscosity data through the Maxwell relationship $\eta = \tau_{shear} \times G_\infty$, where η is the viscosity, τ_{shear} is the shear relaxation time, and G_∞ is the infinite frequency shear modulus.[5] This indicates that the underlying relaxation mechanism for melt enthalpy, melt volume, and melt viscosity is the same. However, most relaxation studies have probed structural relaxation indirectly, i.e., not with a structural probe but by interpreting the variations of a macroscopic property as a function of temperature and time.

Nuclear magnetic resonance (NMR) and Raman spectroscopy have shown that the structure of silicate melts and glasses consists of silica tetrahedra, Q^n ($n=0-4$), where n is the number of bridging oxygens cross-linking the silica tetrahedra and $4-n$ is the number of nonbridging oxygens.[6] The total number of nonbridging oxygens is controlled by the glass composition, i.e., by the amount of mono- and divalent cations available to balance the negative charge of the nonbridging oxygens. The abundance of the Q^n species is controlled by how these nonbridging oxygens are distributed in the structure and follows a set of temperature dependent equilibrium reactions:[7–15]

$$2Q^i \Leftrightarrow Q^{i+1} + Q^{i-1} \quad (\text{for } i = 1-3). \tag{1}$$

For temperatures well above the glass transition, *in situ*, high-temperature NMR has shown that the time scales for viscous flow correspond to the exchange frequency of the Q^n species.[16–19] This led to the conclusion that, at least at these temperatures, Si—O bonds are being broken during viscous flow. However, for temperatures closer to the glass transition, the structural relaxation is too slow to be monitored by high-temperature NMR spectroscopy.

In the present study, we use *in situ*, high-temperature Raman spectroscopy to investigate the relaxation of the silicate network structure around the glass transition. We monitor the temperature and time dependent changes in the intensity of the peaks related to the different silicate species and ring structures, either isothermally after a rapid change in temperature or during constant rate heating and cooling through the glass transition.

II. EXPERIMENT

Two binary potassium silicate melts with 29.4 and 33.3 mol % K_2O were studied by *in situ*, high-temperature Raman spectroscopy. These samples are part of a larger set that was previously investigated by NMR (Ref. 13) and Raman spectroscopy.[14,20] Samples were prepared from reagent grade SiO_2 and K_2CO_3, 0.1 wt % of Fe_2O_3 was added to the samples for the ^{29}Si NMR measurements.[13] *In situ*, high-temperature Raman spectra were collected with a custom-made wire-loop heating stage.[14,21] The temperature was calibrated by melting compounds with known melting points. Laser heating of silicate melts has been observed by Daniel *et al.*[22] to increase the sample temperature at high temperature. However, no laser heating was observed for temperatures below 1800 K by these authors. They explained the absence of laser heating at lower temperature to be due to lack of absorption centers, i.e., broken bond defects, at lower temperatures. At the start of each experiment, the sample was molten into place and quenched to room temperature by switching of the power. The cooling rate around the glass transition was estimated to be ~150 K/s from the times required for crystallization of NaCl, KI, KNO_3, and urea liquids after quenching. The uncertainty on the quench rate is quite large (up to a factor of 2), but this is still small compared to the large difference in cooling rate for the slow and fast quenched samples (by a factor of 1000) or compared to the large range in relaxation times. The Raman spectra were collected with a confocal LabRam system in backscatter geometry, using the 488 nm line of an external argon laser with typically 330 mW on the sample surface. Spectra were collected with two acquisitions of 30 s each. The spectral background was removed by fitting a second order polynomial to the spectral region of 1250–1800 cm^{-1}, where no Raman peaks are present, extrapolating the polynomial to lower frequencies and subtracting it from the spectrum (Fig. 1). This empirical background removal was applied because it results in the highest reproducibility for different spectra of the same sample.[20] Subsequently, a temperature-frequency correction[23] was applied and the spectra were scaled to a maximum intensity of 100.

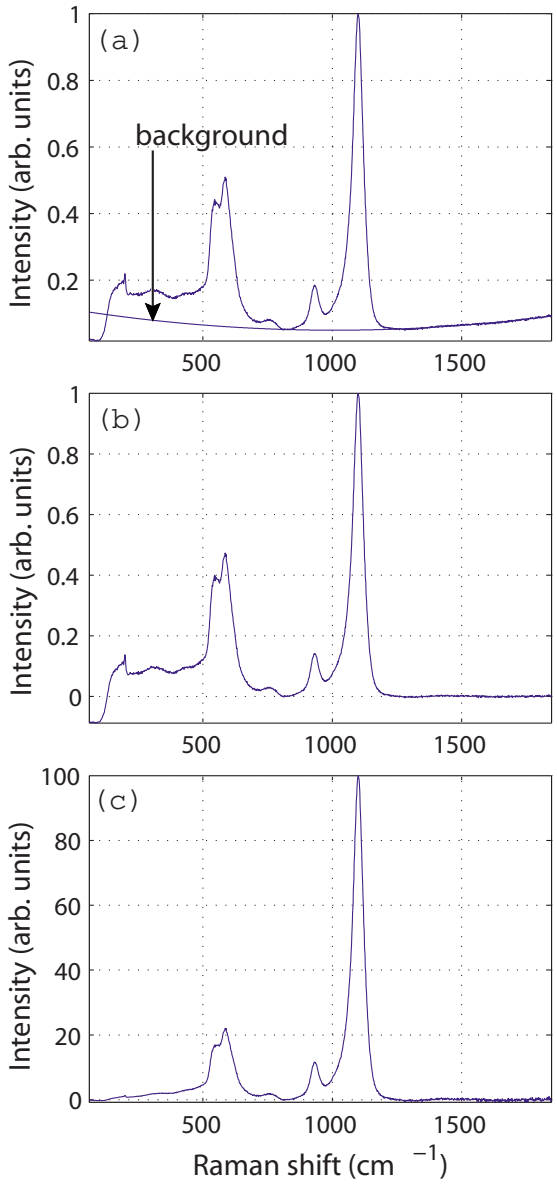

FIG. 1. (Color online) (a) Uncorrected, room-temperature Raman spectrum of potassium disilicate glass (33.3 mol % K_2O). The background was determined by fitting a second order polynomial to the spectral region between 1250 and 1800 cm^{-1}, where no Raman signal is present; (b) background corrected spectrum; (c) temperature-frequency corrected spectrum.

III. RESULTS

The wave number region between 850 and 1200 cm^{-1} contains the stretching vibrations of the different Q^n species (Fig. 2). In the binary K_2O-SiO_2 system, the band at ~925 cm^{-1} has been assigned to a Q^2 vibration, based on the changing band intensities as a function of composition and on the comparison with the spectra of the corresponding crystal phases, e.g., Refs. 8, 9, 11, and 24. In addition, this assignment has been confirmed experimentally[14,20] and by calculations of the vibrational density of state for related compositions.[25,26] The band at ~1100 cm^{-1} is the superposition of vibrations of Q^2, Q^3, and Q^4.[14,20,26] Changes in the relative peak intensities in this spectral region are due to changes in the abundance of the Q^n-species. The band intensity at 925 cm^{-1} can thus be used to monitor the relaxation of the Q^n speciation, and hence the silicate network directly. Because the direct quantification of the speciation from a single Raman spectrum at a given temperature is not possible,[20] the relative peak height itself, and not the Q^2 abundance, will be used as a parameter to monitor the relaxation.

In the first set of experiments, Raman spectra were collected during constant rate heating. The Raman spectra from such a heating run of a fast quenched potassium disilicate glass (33.3 mol % K_2O) in the temperature range of 600–1000 K are shown in Fig. 2. The intensity of the 925 cm^{-1} band is fairly constant below the glass transition (~800 K), decreases on approaching the glass transition, and increases above the glass transition. These changes in peak intensity reflect the changes in the abundance of Q^2 as a function of temperature. This increased abundance of Q^2 with increasing temperature results from a shift of reaction (1) to the right, i.e., Q^3 is replaced by equal amounts of Q^2 and Q^4.[14]

The maximum Raman intensity around 925 cm^{-1} during constant rate heating is plotted as a function of temperature in Fig. 3(a) for samples quenched with two different cooling rates. Similar plots have been obtained for the 29.4 mol % K_2O sample. Similar albeit more noisy results have been obtained when the peak area is plotted rather than the peak height. Whereas the peak area is constant below 720 K (not shown), the peak height decreases in this temperature range [Fig. 3(a)] due to the broadening of the peak. The fictive temperature of the samples during the heating run is obtained by projecting the data in Fig. 3(a) along the sub-T_g slope onto the fit through the points at equilibrium [Fig. 3(b)]. The fictive temperature changes by ~40 K for a difference in quench rate of 3 orders of magnitude [Fig. 3(b)].

In the second set of experiments, the Raman intensity was monitored isothermally as a function of time after a fast temperature step from well below the glass transition into the glass transition region. The starting glasses for those experiments were rapidly quenched glasses (quench rate of 150 K/s) and the observed structural changes represent a relaxation from a high fictive temperature (T_f), i.e., a high apparent equilibrium temperature, toward a lower T_f after the temperature jump into the glass transition region. The maximum Raman intensity at ~925 cm^{-1} is shown as a function of time in Fig. 4. It has been shown that the isothermal relaxation rate depends both on the actual and on the fictive temperature.[27,28] However, the signal to noise ratio is lower for the Raman data than for data on physical properties, and it is not sufficient to simultaneously extract the effect of both the actual and the fictive temperature on the relaxation time. In any case, the influence of the fictive temperature on the relaxation time is small in comparison to the strong dependence of the actual temperature. We have thus proceeded without taking the fictive temperature into account. The data in Fig. 4 can be reproduced well with an exponential decay ($y=y_0+ae^{-x/t}$). Fitting with a stretched exponential function ($y=y_0+ae^{-(x/t)^\beta}$ with $0.5<\beta<1$), as often done in relaxation

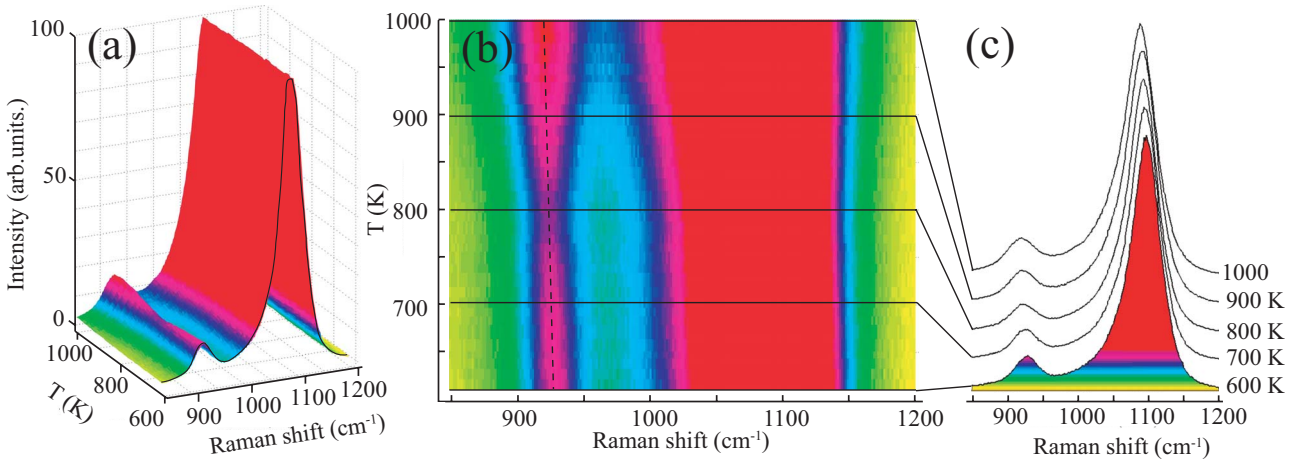

FIG. 2. (Color online) Raman intensity as a function of Raman shift and temperature for a fast quenched, 33.3 mol % K_2O sample: (a) three-dimensional plot, (b) intensity map, and (c) individual spectra for different temperatures. Raman spectra were collected at ~15 K intervals, with an overall heating rate of ~10 K/min. The intensity of the band at ~925 cm^{-1} is fairly constant below the glass transition range (~720–800 K), decreases on approaching the glass transition, and increases above the glass transition. The decrease in intensity upon approaching the glass transition results from the slow heating rate compared to the quench rate. In other words, during the slow heating, sufficient time was available for the structure to relax toward its equilibrium state.

studies,[29,30] yielded $\beta=1$, i.e., a simple exponential function. The relaxation times corresponding to the exponential fit are marked in Fig. 4.

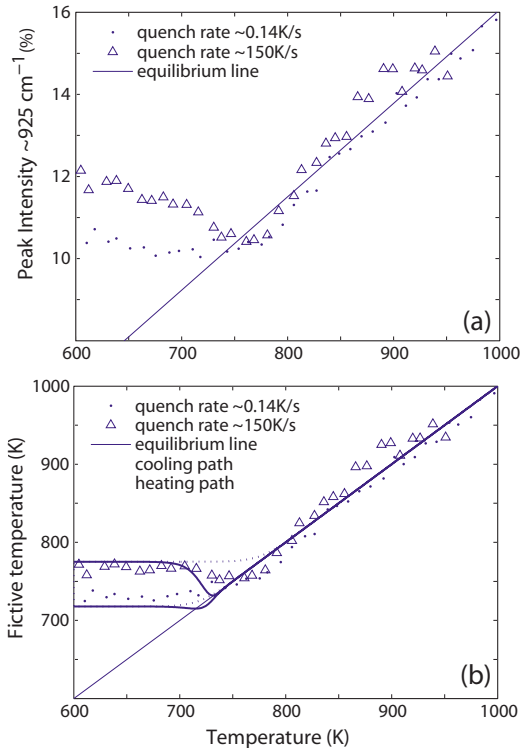

FIG. 3. (Color online) (a) Peak maxima for the ~925 cm^{-1} region as a function of temperature during constant rate heating (0.14 K/s). (b) Fictive temperature as a function of the actual temperature; T_f is obtained by projecting the data in Fig. 3(a) along the sub-T_g slope onto the fit through the point at equilibrium. The cooling and heating curves that are calculated from the viscosity data for the respective quench and heating rates are also plotted.

In order to compare the structural relaxation time with the viscosity in the glass transition region, we calculated the viscosity using the Maxwell relationship $\eta=\tau_{shear}\times G_\infty$, where we have substituted the shear relaxation time τ_{shear} by the structural relaxation times obtained from Raman spectroscopy. Dingwell and Webb[31] have shown that, compared to the large variations in the viscosity, the infinite frequency shear modulus G_∞ can be considered constant for silicate melts: $\log_{10} G_\infty=10\pm0.5$ Pa. It can be seen from Fig. 5 that the obtained viscosities agree well with measured viscosities from literature.[32–34] Thus, the time scales for viscous flow and the relaxation of the speciation to its equilibrium state are the same.

IV. DISCUSSION

Constant rate heating experiments and differential scanning calorimetry, in particular, have long been used to study relaxation kinetics. Despite the striking similarity between Fig. 3(b) and the T_f versus T plots obtained from calorimetry,[30] the methods developed to extract structural relaxation times from calorimetric rate heating data cannot be applied directly to our Raman data because of the higher uncertainties on the Raman data, i.e., the noise in Fig. 3(b). As an alternative, we have calculated the T_f versus T curves using the shear relaxation times obtained from the viscosity data.[32–34] For each time step Δt, we have calculated the fictive temperature $Tf_{(t+\Delta t)}$ as a function of the previous fictive temperature $Tf_{(t)}$, the actual temperature $T_{(t+\Delta t)}$ and the shear relaxation time $\tau_{(t+\Delta t)}$ obtained from viscosity data[32–34] according to the following formula:

$$Tf_{(t+\Delta t)} = Tf_{(t)} + (T_{(t+\Delta t)} - Tf_{(t)})(1 - e^{-\Delta t/\tau_{(t+\Delta t)}}). \quad (2)$$

The calculated cooling and heating curves for the appropriate quench and heating rates are plotted in Fig. 3(b). There is

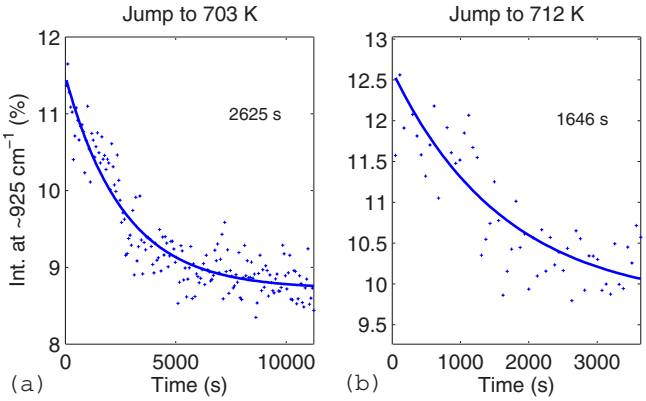

FIG. 4. (Color online) Peak maxima for the ~925 cm^{-1} region as a function of time after a fast temperature step from below T_g into the glass transition range: (a) from 575 to 703 K and (b) from 592 to 712 K; points mark the data; the line is an exponential fit through the data ($y=y_0+ae^{-x/t}$); the corresponding relaxation times t are marked in the figure. As expected, relaxation is slower at 703 K than at 712 K.

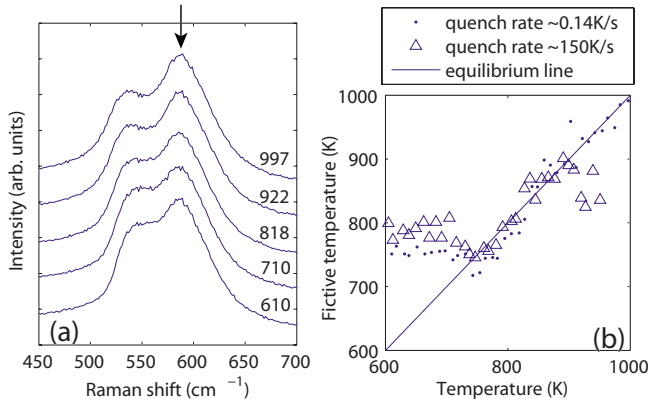

FIG. 6. (Color online) (a) Selected Raman spectra for the 450–700 cm^{-1} spectral region. The arrow indicates the peak assigned to three-membered rings. (b) Fictive temperature as a function of the actual temperature for glasses prepared with different quench rates. The fictive temperatures have been obtained from the intensity of the peak assigned to three-membered rings.

good agreement between the positions and general shapes of the experimental (from Raman spectroscopy) and calculated curves (from viscosity data).

In one direction, using existing viscosity data allows for the calculation of the structural relaxation curves for constant rate cooling and heating [Fig. 3(b)], while in the other direction, the step heating experiments enable the prediction of the viscosity from structural information, i.e., the Q^n speciation (Fig. 5). Since a change in Q^n speciation inevitably involves the breaking of Si—O bonds, the agreement between the viscosity calculated from the speciation relaxation and the measured viscosities provides strong evidence that Si—O bonds are being broken during viscous flow. Thus, the rate of Si—O bond breaking is the primary control on silicate melt viscosity. The probability for cooperative rearrangement of the structure as explained by the Adam-Gibbs relaxation theory,[35] i.e., the probability for Si—O bonds to rearrange in such a way that there is actual movement of material forms a major secondary control on melt viscosity.

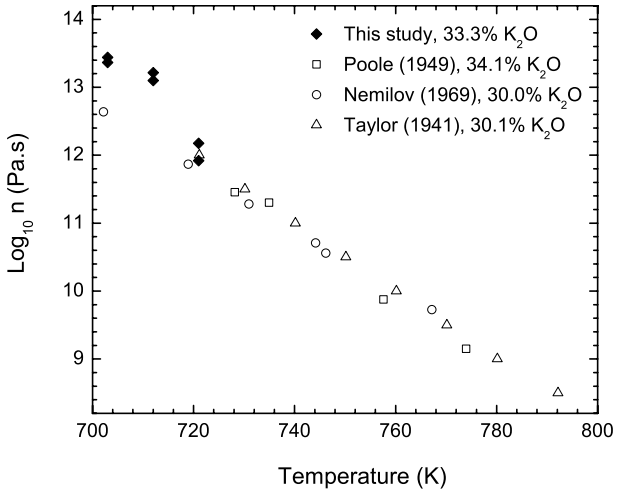

FIG. 5. $\log_{10}\eta$ as a function of temperature for potassium silicate melts (Ref. 32–34). The values obtained from the structural relaxation observed in the Raman spectra (33.3 mol %) are also plotted.

V. MEDIUM-RANGE-ORDER RELAXATION

The wave number region between 450 and 700 cm^{-1} is the range where information on the medium range structure can be extracted [Fig. 6(a)]. In particular, the peak around 585 cm^{-1} has been assigned to breathing vibrations of three-membered rings, i.e., rings consisting of only three SiO_4 tetrahedra, based on, e.g., minimization considerations, classical and *ab initio* calculations of Raman spectra, and comparison to crystalline compounds.[36–43] Recently, we have shown that the intensity of the 585 cm^{-1} peak is related to the number of three-membered rings identified by two-dimensional ^{29}Si NMR spectroscopy.[13] On the other hand, it has been shown that other vibrations may also contribute to the Raman intensity in this spectral region,[44] indicating that the peak areas are not simply proportional to the abundance of the rings. In this study, we do not attempt to quantify the abundance of three-membered rings but use the relative height of the 585 cm^{-1} peak to monitor the relaxation of the medium range order. As for the 925 cm^{-1} peak, fictive temperatures have been obtained from the maximum intensity around 585 cm^{-1} in constant rate heating experiments [Fig. 6(b)]. The relatively large scatter in T_f values obtained from the 585 cm^{-1} peak results from the partial overlap with a peak around 530–550 cm^{-1} and the larger uncertainty on the background removal for this spectral region. The fictive temperature curve obtained from the relaxation of medium range structures [Fig. 6(b)] has the same general shape as the fictive temperature curves obtained from the short range order [Fig. 3(b)]. In both cases, there is a range in T_f of ~40 K for a difference in quench rate of 3 orders of magnitude. However, for a given quench rate, the ring size distribution seems to be frozen in at higher temperature than the Q^n speciation: T_f differs by approximately 15 K. This is not unexpected,

since the rearrangement of the medium range structure involves the breaking of more Si—O bonds than the rearrangement of the Q^n speciation. For silica glass, Levelut *et al.*[45,46] reported a relaxation time of 2400 s at 1448 K for the relaxation of the amplitude of density fluctuations obtained from small angle x-ray scattering intensities. This is 2 orders of magnitude longer than the shear relaxation time calculated with the Maxwell relationship (23 s) from the viscosity at this temperature.[47] This indicates that the time scales for structural relaxation are longer for rearrangements over large length scales than for short length scales.

VI. CONCLUSION

Due to its high sensitivity and relative ease in performing *in situ*, high-temperature measurements, Raman spectroscopy is an ideal technique to probe the relaxation of the short and medium range structures around the glass transition on a molecular level. The rate heating and temperature jump experiments described here can be applied directly to study relaxation processes in a wide range of organic and inorganic glass forming substances. Our results from *in situ* Raman spectroscopy demonstrate that the short to medium range structural rearrangements of the silicate network occur at the same time scale as viscous flow around the glass transition. We showed that the time required for the speciation to equilibrate is equal to the shear relaxation time. Combined with previous results from *in situ* NMR spectroscopy,[16–18] this indicates that, for a viscosity range of 10 orders of magnitude, the mechanism for viscous flow involves the breaking of Si—O bonds. Thus, the rate of Si—O bond breaking is the primary control on silicate melt viscosity.

ACKNOWLEDGMENTS

We would like to thank Urs Menet and Donat Niederer for making the heating stage and Yann Morizet for testing it. Eric Reusser provided access to the Raman facility. Valentina Zakaznova-Herzog and Zoltán Zajacz are thanked for many fruitful discussions. This project was supported by an ETH research grant (0-20168-04) and a Swiss National Science Foundation grant (2-7233-03) to W.H.

[1] C. T. Moynihan, P. B. Macedo, C. J. Montrose, P. K. Gupta, M. A. Debolt, J. F. Dill, B. E. Dom, P. W. Drake, A. J. Easteal, P. B. Elterman, R. P. Moeller, H. Sasabe, and J. A. Wilder, Ann. N.Y. Acad. Sci. **279**, 15 (1976).
[2] P. G. Debenedetti and F. H. Stillinger, Nature (London) **410**, 259 (2001).
[3] C. A. Angell, K. L. Ngai, G. B. McKenna, P. F. McMillan, and S. W. Martin, J. Appl. Phys. **88**, 3113 (2000).
[4] S. L. Webb, R. Knoche, and D. B. Dingwell, Eur. J. Mineral. **4**, 95 (1992).
[5] D. B. Dingwell and S. L. Webb, Eur. J. Mineral. **2**, 427 (1990).
[6] J. F. Stebbins, P. McMillan, and D. B. Dingwell, in *Reviews in Mineralogy*, edited by P. H. Ribbe (Mineralogical Society of America, Washington D.C., 1995), Vol. 32.
[7] M. E. Brandriss and J. F. Stebbins, Geochim. Cosmochim. Acta **52**, 2659 (1988).
[8] B. O. Mysen and J. D. Frantz, Chem. Geol. **96**, 321 (1992).
[9] P. F. McMillan, G. H. Wolf, and B. T. Poe, Chem. Geol. **96**, 351 (1992).
[10] R. Dupree, D. Holland, and D. S. Williams, J. Non-Cryst. Solids **81**, 185 (1986).
[11] S. A. Brawer and W. B. White, J. Chem. Phys. **63**, 2421 (1975).
[12] H. Maekawa, T. Maekawa, K. Kawamura, and T. Yokokawa, J. Non-Cryst. Solids **127**, 53 (1991).
[13] W. J. Malfait, W. E. Halter, Y. Morizet, B. H. Meier, and R. Verel, Geochim. Cosmochim. Acta **71**, 6002 (2007).
[14] W. J. Malfait, V. P. Zakaznova-Herzog, and W. E. Halter, J. Non-Cryst. Solids **353**, 4029 (2007).
[15] W. J. Malfait, V. P. Zakaznova-Herzog, and W. E. Halter, Am. Mineral. (to be published).
[16] J. F. Stebbins and I. Farnan, Science **255**, 586 (1992).
[17] S.-B. Liu, J. F. Stebbins, E. Schneider, and A. Pines, Geochim. Cosmochim. Acta **52**, 527 (1988).
[18] I. Farnan and J. F. Stebbins, J. Non-Cryst. Solids **124**, 207 (1990).
[19] I. Farnan and J. F. Stebbins, Science **265**, 1206 (1994).
[20] V. P. Zakaznova-Herzog, W. J. Malfait, F. Herzog, and W. E. Halter, J. Non-Cryst. Solids **353**, 4015 (2007).
[21] J. Ohashi and G. Hadidiacos, Carnegie Inst. Washington Publ. **75**, 828 (1976).
[22] I. Daniel, P. Gillet, B. T. Poe, and P. F. McMillan, Phys. Chem. Glasses **22**, 74 (1995).
[23] D. A. Long, *Raman Spectroscopy* (McGraw-Hill, New York, 1977).
[24] D. W. Matson, S. K. Sharma, and J. A. Philpotts, J. Non-Cryst. Solids **58**, 323 (1983).
[25] Y. Q. Wu, G. C. Jiang, J. L. You, H. Y. Hou, H. Chen, and K. D. Xu, J. Chem. Phys. **121**, 7883 (2004).
[26] N. Zotov, I. Ebbsjö, D. Timpel, and H. Keppler, Phys. Rev. B **60**, 6383 (1999).
[27] O. S. Narayanaswamy, J. Am. Ceram. Soc. **54**, 491 (1971).
[28] A. Q. Tool, J. Am. Ceram. Soc. **29**, 240 (1946).
[29] R. Bohmer, K. L. Ngai, C. A. Angell, and D. J. Plazek, J. Chem. Phys. **99**, 4201 (1993).
[30] M. A. Debolt, A. J. Easteal, P. B. Macedo, and C. T. Moynihan, J. Am. Ceram. Soc. **59**, 16 (1976).
[31] D. B. Dingwell and S. L. Webb, Phys. Chem. Miner. **16**, 508 (1989).
[32] N. W. Taylor and R. F. Doran, J. Am. Ceram. Soc. **24**, 103 (1941).
[33] J. P. Poole, J. Am. Ceram. Soc. **32**, 230 (1949).
[34] S. V. Nemilow, Zh. Prikl. Khim. (S.-Peterburg) **42**, 55 (1969).
[35] G. Adam and J. H. Gibbs, J. Chem. Phys. **43**, 139 (1965).
[36] P. Umari, X. Gonze, and A. Pasquarello, Phys. Rev. Lett. **90**, 027401 (2003).
[37] P. Umari and A. Pasquarello, Physica B **316**, 572 (2002).
[38] J. Choisnet, A. Deschanvres, and P. Tarte, Spectrochim. Acta, Part A **31A**, 1023 (1975).

[39] R. Elliott, J. Non-Cryst. Solids **182**, 1 (1995).
[40] F. L. Galeener, Solid State Commun. **44**, 1037 (1982).
[41] F. L. Galeener, R. A. Barrio, E. Martinez, and R. J. Elliott, Phys. Rev. Lett. **53**, 2429 (1984).
[42] J. D. Kubicki and D. Sykes, Phys. Chem. Miner. **19**, 381 (1993).
[43] D. A. McKeown, M. I. Bell, and C. C. Kim, Phys. Rev. B **48**, 16357 (1993).
[44] A. Rahmani, M. Benoit, and C. Benoit, Phys. Rev. B **68**, 184202 (2003).
[45] C. Levelut, A. Faivre, R. Le Parc, B. Champagnon, J.-L. Hazemann, L. David, C. Rochas, and J.-P. Simon, J. Non-Cryst. Solids **307-310**, 426 (2002).
[46] C. Levelut, R. Le Parc, A. Faivre, and B. Champagnon, J. Non-Cryst. Solids **352**, 4495 (2006).
[47] G. Urbain, Y. Bottinga, and P. Richet, Geochim. Cosmochim. Acta **46**, 1061 (1982).